

Hydrodynamic source with continuous emission in Au+Au collisions at $\sqrt{s} = 200$ GeV

M. S. Borysova,¹ Yu. M. Sinyukov,² S. V. Akkelin,² B. Erasmus,³ and Iu. A. Karpenko^{1,2}

¹Taras Shevchenko National University, Kiev 01033, Volodymirs'ka 64, Ukraine

²Bogolyubov Institute for Theoretical Physics, Kiev 03143, Metrologichna 14b, Ukraine

³SUBATECH (UMR, Université, Ecole des Mines, IN2P3/CNRS), 4, rue Alfred Castler, F-44070 Nantes Cedex 03, France

(Received 31 August 2005; published 28 February 2006)

We analyze single-particle momentum spectra and interferometry radii in central Au+Au collisions at RHIC within a hydro-inspired parametrization accounting for continuous hadron emission through the whole lifetime of hydrodynamically expanding fireball. We found that a satisfactory description of the data is achieved for a physically reasonable set of parameters when the emission from non-space-like sectors of the enclosed freeze-out hypersurface is fairly long: 9 fm/c. This protracted surface emission is compensated in outward interferometry radii by positive $r_{\text{out}} - t$ correlations that are the result of an intensive transverse expansion. The main features of the experimental data are reproduced: in particular, the obtained ratio of the outward to sideward interferometry radii is less than unity and decreases with increasing transverse momenta of pion pairs. The extracted value of the temperature of emission from the surface of hydrodynamic tube approximately coincides with one found at chemical freeze-out in RHIC Au+Au collisions. A significant contribution of the surface emission to the spectra and to the correlation functions at relatively large transverse momenta should be taken into account in advanced hydrodynamic models of ultrarelativistic nucleus-nucleus collisions.

DOI: [10.1103/PhysRevC.73.024903](https://doi.org/10.1103/PhysRevC.73.024903)

PACS number(s): 25.75.Gz, 25.75.Ld

I. INTRODUCTION

It is quite possible that a new state of matter is created at unprecedented high-energy density reached in relativistic heavy-ion collisions at RHIC [1]. This conclusion is based, in particular, on the success of hydrodynamic models in description of the measured single-particle hadron momentum spectra and elliptic flows [2]. Within the hydrodynamic approach, there is, in principle, a possibility to extract the equation of state (EoS) of the thermalized system and then get information about the early stage of the collision processes and even the type of the phase transition between QGP and the hadron matter.

However, quantitative determination of the EoS in the hydrodynamic approach is a nontrivial problem. It depends on both the initial conditions and system “freeze-out” prescription. The latter determines the final conditions of hydrodynamic expansion: one cannot use hydrodynamic equations for infinitely large times because the resulting very small densities destroy the picture of continuous medium of real particles. Usually, the freeze-out hypersurface that confines the four-volume of hydrodynamic evolution is included as an external input with respect to hydrodynamic equations. Then, typically, particle spectra are described by the Cooper-Frye prescription (CFp) [3], which treats freeze-out as a sudden transition from local thermal equilibrium to free streaming that happens on some spacelike 3D hypersurface, e.g., on a space-like part of the isotherm: $T \simeq m_\pi$ [4]. In reality the process of freeze-out, or particle liberation, is quite complicated because the particles escape from the system during the whole period of its evolution (see, e.g., Ref. [5]). A method that is based on Boltzmann equation was recently proposed in Ref. [6] to describe the spectra formation in the hydrodynamic approach to $A+A$ collisions using the escape probabilities. The region of applicability of CFp and its possible generalizations are

discussed there, as well as in Ref. [7]. In present work we do not consider the whole complexity of the freeze-out process (see, e.g., Refs. [6–9]). Instead we account for continuous (in time) emission process by applying the generalized Cooper-Frye prescription for an *enclosed* freeze-out hypersurface. Such an enclosed hypersurface contains spacelike sectors of the volume emission and non-space-like ones (with space-like normal) of the surface emission.

It is well known [10] that protracted surface emission may lead to the ratio of the outward to sideward interferometry radii, $R_{\text{out}}/R_{\text{side}}$, much bigger than unity for typical scenarios of phase transition in heavy-ion collisions [11]. These expectations are, however, in contradiction with current experimental data from RHIC where $R_{\text{out}}/R_{\text{side}} \simeq 1$ (see, e.g., Ref. [12]). This discrepancy is a component of the so-called HBT puzzle [13]. Naively, from this one might conclude that the duration of emission is very short. However, the $R_{\text{out}}/R_{\text{side}}$ ratio is also quite sensitive to the shape of freeze-out hypersurface because, unlike R_{side} , R_{out} is a mixture of the *out* width, time spread of emission, and the $r_{\text{out}} - t$ correlations. Indeed, in the Gaussian approximation for the correlation function the interferometry radii can be expressed in terms of the space-time variances¹ (see, e.g., Ref. [14]):

$$R_i^2(p) = \langle (\Delta r_i - v_i \Delta t)^2 \rangle_p \\ = \langle \Delta r_i^2 \rangle_p + v_i^2 \langle \Delta t^2 \rangle_p - 2v_i \langle \Delta r_i \Delta t \rangle_p, \quad (1)$$

where $v_i = p_i/p_0$, p_i , r_i ($i = \text{out, side, long}$) are the Cartesian components of the vectors \mathbf{v} , \mathbf{p} , and \mathbf{r} , respectively, and

¹Note that if the distribution function has a non-Gaussian form, which is typical for expanding sources, then the expression of the interferometry radii through space-time variances can be associated with the behavior of the correlation function at small $q = p_1 - p_2 \rightarrow 0$ only and, therefore, could be used solely for qualitative estimates.

$p^\mu = (p_0, p_{\text{out}}, 0, p_{\text{long}})$ is the mean four-momentum of the two registered particles. Here $\Delta r_i = r_i - \langle r_i \rangle_p$, $\Delta t = t - \langle t \rangle_p$, and $\langle \dots \rangle_p$ denotes the averaged (over the distribution function) value taken at some momentum p . Note that in the Bertsch-Pratt reference frame [15] $p_{\text{side}} = 0$ and therefore $p_{\text{out}} = p_T$, where p_T is the absolute value of the transverse component of the vector \mathbf{p} . It is easy to see from Eq. (1) that positive $r_{\text{out}} - t$ correlations, $\langle \Delta r_{\text{out}} \Delta t \rangle_p > 0$, give a *negative* contribution to R_{out} reducing thereby the $R_{\text{out}}/R_{\text{side}}$ ratio.² Therefore one can conclude that relatively small $R_{\text{out}}/R_{\text{side}} \simeq 1$ ratio in a case of a prolonged surface emission can take place if there are positive $r_{\text{out}} - t$ correlations in the corresponding sector of the freeze-out hypersurface. Such a sector has typically a space-like four-normal. Then an interval between space-time points in such a sector can be, generally, spacelike as well as timelike. Although the bulk of hadrons are emitted from the sector with a time-like normal (volume emission), the surface emission from the sector with a space-like normal can be, nevertheless, important for spectra and HBT radii formation,³ especially at relatively high p_T . A difference in temperature values and intensities of collective flows⁴ in different freeze-out sectors can increase the effect, and thus a consistent description of the single-particle spectra and interferometry radii can be reached in hydrodynamically motivated models with an enclosed freeze-out hypersurface that accounts for continuous (in time) character of particle emission.

It is well known that when the freeze-out hypersurface σ has non-space-like sectors, the CFP is inconsistent. Then the CFP should be modified to exclude formally negative contributions to the particle number at the corresponding momenta. The simplest prescription is to present the distribution function as a product of a local thermal distribution and the step function such as $\theta[p_\mu n^\mu(x)]$ [19,20], $n^\mu n_\mu = \pm 1$, where n^μ is a time-like or space-like outward normal to a freeze-out hypersurface σ .⁵ Thereby freeze-out is restricted to those particles for which $p_\mu n^\mu(x)$ is positive.

Sometimes, to avoid the above-mentioned problems with CFP, the continuity of particles emission in heavy-ion collisions is taken into account by means of the emission (source) function $S(x, p)$ (see, e.g., Ref. [14]), which is used instead of the distribution (Wigner) function $f(x, p)$ in some hydro-inspired parameterizations and is usually chosen to be proportional to the local equilibrium distribution function, $f_{l.eq}(x, p)$, with a smearing (proper) time factor $\exp[-(\tau - \tau_0)^2/\Delta\tau^2]$. First, such a prescription loses an extremely important information about $\tau - r_i$ correlations: It is naturally that at early times the emission function is concentrated

mostly at the periphery of the system on the boundary with vacuum, because particles cannot escape from the hot and dense central region. The approximation of surface emission is, thus, much more realistic for the early times. Second, although the distribution function is well defined for a given state of the system, as the local Bose-Einstein or Fermi-Dirac distributions are associated with a locally equilibrated state, $S(x, p)$ is much more complicated and model dependent [7,21]. It is demonstrated in Ref. [6], starting from a particular exact solution of the Boltzmann equation, that the emission function is not proportional to the local equilibrium distribution (Wigner function), although the system is in a local equilibrium state. Therefore, the widely used (see, e.g., so called “blast-wave” model [22]) “local equilibrium” ansatz, $S \sim f_{l.eq.}$, is supported neither by analytic kinetic results nor numerical transport calculations except for the formal case when all the particles are emitted simultaneously: The emission function is then the distribution function multiplied by a Δ function concentrated on the freeze-out hypersurface. Perhaps too large values of maximal collective velocities, close to the speed of light, which are necessary to fit the spectra in the blast-wave parametrization, and a failure in fitting HBT radii (especially R_{side} , see Refs. [22]) are caused by an improper description of the particle emission process.

The aim of this work is a coherent description of pion, kaon, and proton single-particle momentum spectra as well as the HBT pion radii in central RHIC Au+Au collisions at $\sqrt{s_{NN}} = 200$ GeV by means of a simple hydrodynamically motivated parametrization with an enclosed freeze-out hypersurface. As a matter of fact, we generalize the blast-wave parametrization for a realistic case of continuous emission over the whole lifetime of the fireball. We demonstrate that a consistent description of the observables is possible if the freeze-out hypersurface has a non-space-like sector emitting a noticeable part of the particles.⁶ The latter condition is satisfied when particles are emitted from the surface of an expanding hydrodynamic tube soon after the hadronization, which at early times happens at the periphery of the volume occupied by quark-gluon matter.

II. HYDRO-INSPIRED PARAMETRIZATION OF CONTINUOUS HADRONIC FREEZE-OUT IN CENTRAL RHIC AU+AU COLLISIONS

We assume that particles are emitted from some 3D hypersurface when the fireball is in a locally equilibrated (leq) state,

$$f_i = f_{l.eq,i}(x, p) = (2\pi)^{-3} \left\{ \exp \left[\frac{u_\nu(x) p^\nu - \mu_i(x)}{T(x)} \right] \pm 1 \right\}^{-1}, \quad (2)$$

characterized by the temperature $T(x)$ (which is common for all the particle species), collective velocity field $u_\mu(x)$ and the

²This mechanism of reduction of the $R_{\text{out}}/R_{\text{side}}$ ratio is realized in a multiphase transport (AMPT) model [16].

³See the relevant analysis in Ref. [17]

⁴It was found in Ref. [18] that the transport freeze-out process is similar to evaporation: high- p_T particles freeze out early from the surface, whereas low- p_T ones decouple later from the system's center.

⁵If a fluid element that crosses a sector of the freeze-out hypersurface with a space-like normal decays, preserving its total particle number, then this prescription is somewhat more complicated [19].

⁶The importance of surface emission has been stressed also in Refs. [23] for opaque sources that emit particles from a surface layer of finite thickness, then $\langle \Delta r_{\text{out}}^2 \rangle_p < \langle \Delta r_{\text{side}}^2 \rangle_p$ reducing thereby $R_{\text{out}}/R_{\text{side}}$ ratio.

chemical potentials $\mu_i(x)$ depending on the particle species i . We refer to the part of 3D hypersurface with a time-like normal vector as v (volume) freeze-out, or final breakup, and the rest of the hypersurface with a space-like normal as s (surface) freeze-out, corresponding to continuous emission prior to the final breakup. We assume that particle densities are uniform at each v and s hypersurface separately, but, in general, are different from each other. Then the temperature and chemical potential in Eq. (2) are replaced with T_v, T_s and $\mu_{v,i}, \mu_{s,i}$ for the v and s freeze-out sectors, respectively. For the sake of simplicity and reduction of the number of parameters we do not interpolate smoothly the values of temperature and chemical potential between the *volume* and *surface* sectors of the hypersurface. A longitudinally boost-invariant expansion is a rather good approximation in midrapidity region at RHIC [24]; therefore, we assume boost invariance for longitudinal hydrodynamic velocities in this region, $v_L = z/t$, which allows us to parameterize t and z at 3D hypersurface σ as $t_{v,s} = \tau_{v,s}(r) \cosh(\eta)$, $z_{v,s} = \tau_{v,s}(r) \sinh(\eta)$ in both sectors of the freeze-out hypersurface, where $\tau = \sqrt{t^2 - z^2}$ is the Bjorken proper time [25] and η is the longitudinal fluid rapidity, $\eta = \tanh^{-1} v_L$; in addition, r is the absolute value of transverse coordinate $\mathbf{r}_T \equiv (x, y) = (r \cos \phi, r \sin \phi)$. Taking into account the transverse velocity component $v(r, \tau)$ in the longitudinally comoving frame, we obtain for the collective four-velocity

$$u_{v,s}^\mu(r, \eta) = (\cosh \eta \cosh \eta_T^{v,s}, \sinh \eta_T^{v,s} \cos \phi, \sinh \eta_T^{v,s} \sin \phi, \sinh \eta \cosh \eta_T^{v,s}), \quad (3)$$

where $\eta_T^{v,s}(r, \tau_{v,s})$ is the transverse fluid rapidity, $\eta_T = \tanh^{-1} v(r, \tau)$. The particle four-momentum can be expressed through the momentum rapidity y , transverse momentum \mathbf{p}_T

and transverse mass $m_T = \sqrt{m^2 + p_T^2}$,

$$p^\mu = (m_T \cosh y, \mathbf{p}_T, m_T \sinh y). \quad (4)$$

Then

$$\frac{p_\mu u^\mu}{T} = \frac{m_T}{T} \cosh(y - \eta) \cosh \eta_T - \frac{\mathbf{p}_T \cdot \mathbf{r}_T}{T r} \sinh \eta_T. \quad (5)$$

The *volume* and *surface* elements of the freeze-out hypersurface $\sigma(x)$ take the form

$$d\sigma_\mu^{v,s} = n_\mu^{v,s} d\sigma = \pm \tau_{v,s}(r) d\eta dr_x dr_y (\cosh \eta, -d\tau_{v,s}/dr_x, -d\tau_{v,s}/dr_y, -\sinh \eta), \quad (6)$$

where

$$n_\mu^{v,s} = \pm \frac{(\cosh \eta, -d\tau_{v,s}/dr_x, -d\tau_{v,s}/dr_y, -\sinh \eta)}{\{\pm[1 - (d\tau_{v,s}/dr_x)^2 - (d\tau_{v,s}/dr_y)^2]\}^{1/2}}. \quad (7)$$

and $+$ and $-$ correspond to the v and s sectors of the hypersurface respectively.⁷ The surface ‘‘moves’’ with a velocity less than the speed of light, $|dr_s(\tau)/d\tau| < 1$, hence $|d\tau_s(r)/dr| > 1$. If the 2D surface of the 3D s freeze-out sector ‘‘moves’’ outward, $d\tau_s/dr_x, d\tau_s/dr_y > 0$, then the product $p^\mu n_\mu$ will be negative if the p_T of particles are sufficiently small. In that case such particles cannot really escape from the system. For particles with fairly high transverse momenta one has $p^\mu n_\mu > 0$, and they will be emitted from the surface of the system into vacuum and stream freely toward detectors. To take this into account we use a modified Cooper-Frye prescription with the substitution [19,20]

$$f_{leq}(x, p) \rightarrow \theta[p_\mu n^\mu(x)] f_{leq}(x, p) \quad (8)$$

to get the single-particle spectra $p_0 d^3 N/d^3 p$ for diverse particle species and the correlation function of pions $C(p, q)$:

$$p_0 \frac{d^3 N}{d^3 p} = \int p^\mu d\sigma_\mu \theta[p_\mu n^\mu(x)] f_{leq}(x, p) \quad (9)$$

$$C(p, q) = 1 + \frac{|\int p^\mu d\sigma_\mu \theta[p_\mu n^\mu(x)] f_{leq}(x, p) \exp(iqx)|^2}{\{\int p_1^\mu d\sigma_\mu \theta[p_1^\mu n_\mu(x)] f_{leq}(x, p_1)\} \{\int p_2^\mu d\sigma_\mu \theta[p_2^\mu n_\mu(x)] f_{leq}(x, p_2)\}}. \quad (10)$$

Here $p = (p_1 + p_2)/2$, $q = p_1 - p_2$. To calculate the correlation function in the region of correlation peak we utilize the smoothness mass-shell approximation:

$$C(p, q) \approx 1 + \frac{|\int p^{*\mu} d\sigma_\mu \theta[p^{*\mu} n^\mu(x)] f_{leq}(x, p^*) \exp(iqx)|^2}{\{\int p^{*\mu} d\sigma_\mu \theta[p^{*\mu} n_\mu(x)] f_{leq}(x, p^*)\}^2}, \quad (11)$$

where

$$p^{*\mu} = \left(\sqrt{m^2 + \left(\frac{\mathbf{p}_1 + \mathbf{p}_2}{2} \right)^2}, \left(\frac{\mathbf{p}_1 + \mathbf{p}_2}{2} \right) \right).$$

We assume that the source of particles in central Au+Au RHIC collisions has cylindrical symmetry and is strongly stretched out in the beam direction (long direction): The longitudinal size is much larger than the corresponding length of

homogeneity [26,27]. The latter allows us to neglect the finiteness of the system in the longitudinal direction when we calculate particle spectra in the midrapidity region around $y \approx 0$. As for the transverse direction, we assume that the source has a finite geometrical size encoded in the limits of integration over r : $0 < r < R_f$ for v emission and $R_i < r < R_f$ for s emission, where R_i and R_f are the initial and finite effective radii of the system.

To fix a model one needs to define $\tau(r)$ and the transverse rapidity $\eta_T(r)$. We choose the simplest ansatz, aimed at

⁷Note that the above representation of elements of the freeze-out hypersurface $\sigma(x)$ in the s sector is, of course, not unique and is used because of its convenience for the chosen type of $\sigma(x)$ (see below). It should be changed if $dr_s(\tau)/d\tau = 0$ on some part of this hypersurface.

catching the main features of particle emission. We suppose that the *volume* (spacelike) emission happens as assumed in the blast-wave model at the constant $\tau_i(r) = \tau_f$, and the *surface* emission takes place during the whole time of hydrodynamic evolution of system: $\tau_i < \tau_s < \tau_f$, where τ_i is the initial time of thermalization. Because the fireballs formed in RHIC collisions expand in transverse direction with rather high transverse velocity, we can assume that $d\tau_s(r)/dr > 0$ for the *surface* freeze-out.⁸ For the sake of simplicity we parameterize $\tau_s(r)$ by a linear function,

$$\tau_s(r) = a \cdot r + b. \quad (12)$$

Taking into account that $\tau_s(R_i) = \tau_i$ and $\tau_s(R_f) = \tau_f$, where R_i and R_f are the initial and final transverse radii, respectively, $R_i < R_f$, we obtain that

$$a = \frac{\tau_f - \tau_i}{R_f - R_i}, \quad (13)$$

$$b = \tau_i - \frac{\tau_f - \tau_i}{R_f - R_i} R_i. \quad (14)$$

Please note that the chosen form of $\tau_s(r)$ is just an approximation that reflects the main properties of the *surface* freeze-out. For example, the chosen constant velocity of outward motion of the transverse surface, $1/a$, is associated with the mean (averaged over time) velocity of the surface, which generally can move with time-dependent velocity.

The form of freeze-out $\tau(r)$ is presented in Fig. 1. It is convenient to parameterize the *volume* as well as *surface* sectors of the 3D hypersurface by r_T and longitudinal rapidity η , therefore the integration in Eqs. (9) and (11) is carried out separately for those sectors: $\int d\sigma_\mu[\dots] \rightarrow \int d\sigma_\mu^v[\dots]_v + \int d\sigma_\mu^s[\dots]_s$.

To specify the transverse rapidity $\eta_T(r)$, we first connect smoothly the values of transverse rapidity in the *volume* and *surface* sectors of the hypersurface on their ‘‘border.’’ Second, because a linear r dependence of the radial velocity profile was found in hydrodynamic simulations [29] for small transverse collective velocities $v \approx \eta_T$ near the center of the system at fixed τ , we assume that the transverse flow rapidity profile depends linearly on r for *volume* freeze-out at $\tau = \tau_f$,

$$\eta_T^v(r, \tau_f) = \eta_T^{\max} \frac{r}{R_f}, \quad (15)$$

where η_T^{\max} is the maximal transverse rapidity of the fluid. As for the transverse rapidity profile in the *surface* sector of the freeze-out hypersurface, we analyzed various parameterizations. Fits to the data prefer a nonzero initial transverse velocity at $\tau_i = 1 \text{ fm/c}$, which is physically reasonable. Indeed, it seems to be natural that the transverse flow velocity at freeze-out surface at any time (or, at least, on average) should not be smaller than the average ‘‘velocity’’ of the surface, $1/a$. Such an ‘‘initial’’ velocity, $v_T(\tau_i = 1 \text{ fm/c})$, can be developed even

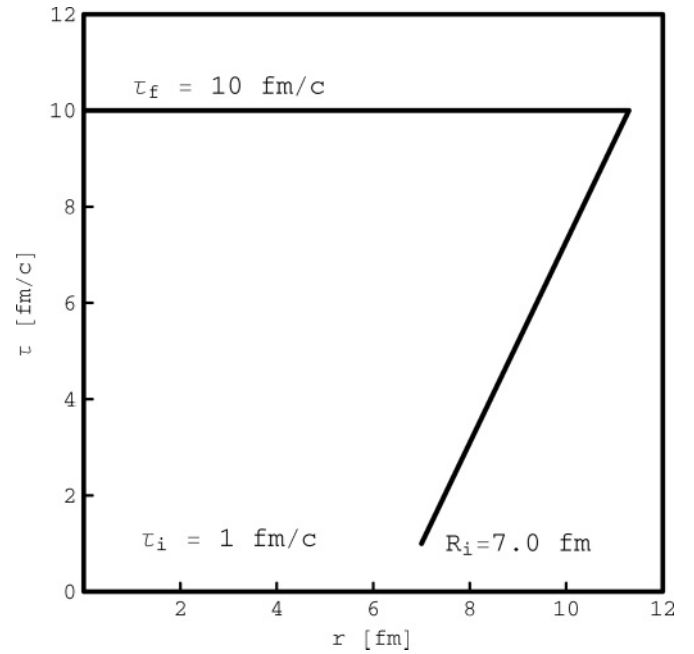


FIG. 1. The enclosed freeze-out hypersurface $\tau(r)$. See the text for details.

at the nonthermal partonic stage before τ_i . Also a nonzero initial velocity does not contradict an approximate linearity with radius of rapidity profile at early times, in particular at τ_i . One of the simplest parametrizations that satisfies these properties and allows us to connect smoothly the values of transverse rapidity in the *volume* and *surface* sectors is the following transverse rapidity distribution:

$$\eta_T^s[r, \tau_s(r)] = \eta_T^{\max} \frac{\sqrt{[\tau_s(r) - \tau_i]^2 + r^2}}{\sqrt{(\tau_f - \tau_i)^2 + R_f^2}}. \quad (16)$$

Note that $\tau_s(R_f) = \tau_f$ and $\eta_T^s[R_f, \tau_s(R_f)] = \eta_T^v(R_f, \tau_f) = \eta_T^{\max}$.

In the next section we apply our model to description of pion, kaon, and proton transverse-momentum spectra and pion interferometry radii in midrapidity in RHIC Au+Au central collisions at $\sqrt{s_{NN}} = 200 \text{ GeV}$.

III. RESULTS AND DISCUSSION

We assume a common enclosed freeze-out hypersurface for all particles species. Then the model contains seven parameters: $\tau_i, \tau_f, R_i, R_f, T_v, T_s, \eta_T^{\max}$. As commonly accepted, we assume that at $\tau_i = 1 \text{ fm/c}$ the system is already in local thermal equilibrium, and so we do not consider this value as a free parameter.

The values of chemical potentials $\mu_{s,j}, \mu_{v,j}$ that are different for different particle species j , are not free parameters and are responsible for the absolute normalization of the spectrum. In details, the situation is somewhat more complicated because resonance decays contribute to both the particle spectra and interferometry radii [30]. About 1/2–2/3 of pions, kaons, and protons come from those decays after chemical freeze-out

⁸This is in full correspondence with the form of the hypersurface of constant densities (particle number and energy) in analytic ellipsoidal solutions of relativistic hydrodynamics [28]. It seems that initial or fast developed transverse velocities are required to provide a positive $t - r$ correlation in s sector of freeze-out hypersurface.

TABLE I. Model parameters from fits of Au+Au $\sqrt{s_{NN}} = 200$ GeV data on π^- , K^- , and p single-particle spectra and π^- HBT radii. The ratio of detected particle numbers to thermal (primary) ones (last column) as well as μ_s for pions and kaons were kept constant during fit procedures.

	μ_v (MeV)	μ_s (MeV)	$(dN^{\text{reg}}/dy)/(dN^{\text{th}}/dy)$
π^-	53	0	2.2
K^-	45	0	2.2
p	280	40	3.5

happens in high-energy heavy-ion collisions [27,31,32]. The corresponding contribution to pion spectra and interferometry radii was estimated in Ref. [33] within the hydrodynamic model developed in Ref. [27]. According to the results of Ref. [33], resonance decays do not change significantly the slopes of the transverse pion spectra in the region of interest for kinetic freeze-out temperatures T_v and flows at RHIC collisions. Note that the resonance emission from the surface is negligible because heavy resonances have too small heat velocities to escape from the expanding system. As for the pion interferometry radii, the decays of short-lived resonances result in an augmentation of them as compared with the picture of pure thermal emission, especially in the region of small p_T . This resonance contribution to the pion interferometry radii decreases with the increase of transverse momenta of the pairs and, as it was found in Ref. [33], is smaller than 6%–14% for $p_T > 0.3$ GeV (see also Ref. [34]).

Based on these studies, we neglect the changes of slopes of particle transverse spectra because of resonance decays and fit the pion interferometry radii starting from $m_T \simeq 0.3$ GeV where the resonance contributions are fairly small. Finally, to fix $\mu_{v,j}$, $\mu_{s,j}$ for thermal (primary) particles at some T_v and T_s , one needs to know what fraction of measured particles is produced by resonances after thermal (kinetic) freeze-out. Such a problem is not fully solved until now and needs further analysis. Because the main aim of this article is to describe the main features of the physical picture of particle emission in central RHIC Au+Au collisions rather than to fine-tune the parameters and perfectly describe the data, we fit the fraction of thermal (direct) particles within reasonable limits discussed above; our final choice is presented in the last column of Table I.

A preliminary analysis shows that a good fit to spectra and correlations formed on an enclosed hypersurface cannot be obtained if the *surface* temperature T_s is taken within the standard range for kinetic freeze-out: $100 \text{ MeV} \leq T_s \leq m_\pi$; it should be taken higher than the pion mass m_π .⁹ It forces us to conclude that the temperature of surface emission is close to the chemical freeze-out temperature, or the hadronization one if chemical freeze-out happens at about the same time,

⁹The same conclusion that the best fit of the pion HBT radii is obtained when the temperature of *surface* emission from a hypersurface with a spacelike normal is significantly higher than the temperature of *volume* emission is made also in Ref. [35], where SPS data for 158A GeV central Pb+Pb collisions are analyzed.

TABLE II. Model parameters from fits of Au+Au $\sqrt{s_{NN}} = 200$ GeV data on π^- , K^- , and p single-particle spectra and π^- HBT radii. The value of τ_i was kept constant through fit procedures.

	τ_i (fm/c)	τ_f (fm/c)	R_i (fm)	R_f (fm)	T_v (MeV)	T_s (MeV)	η_T^{max}
π^-, K^-, p	1	10	7	11.3	110	150	0.73

as it is argued in Ref. [36]. Because the periphery of an expanding system is more dilute, the matter there is in the hadronic phase and hadrons can easily escape from this layer into the surrounding vacuum despite the relatively high temperature; this was argued in detail in Ref. [19]. This natural picture of surface emission at earlier times $\tau_s < \tau_f$ gives us a possibility to assume $\mu_s = 0$ for pions and kaons, accounting for chemical equilibrium of pions at chemical freeze-out (see, e.g., Ref. [32]) and almost zero net strangeness in central RHIC Au+Au collisions at the top energy. The results of our fit, which are presented in Tables I and II, demonstrate that the best fit fixes the value of T_s at 150 MeV, which is indeed very close to the chemical freeze-out temperature 157 ± 3 MeV obtained in Ref. [37]. This justifies our assumption *a posteriori*. The best fit to proton transverse spectra is achieved at $\mu_{s,p} = 40$ MeV, which is slightly more than the value $\mu_B = 28.2 \pm 3.6$ MeV found in Ref. [37] for the baryochemical potential.¹⁰ Concerning the values $\mu_{v,j}$, one readily sees that they are not free parameters of the model, because they should be fixed by the measured respective rapidity densities, dN_j/dy .

The best fit to data is obtained for the parameters shown in Tables I and II. We also present there parameters that were kept constant through the fit procedure. As one can see from Figs. 2–4 and Tables I and II, that good description of pion, proton, and kaon spectra and pion interferometry radii is achieved in the midrapidity region of central $\sqrt{s_{NN}} = 200$ GeV Au+Au collisions. The STAR collaboration data are presented for illustration. We did not fit these data because they are limited to relatively small p_T values as compared to the PHENIX data, whereas the surface emission gives a significant contribution in the region of high transverse momenta. It is noteworthy, that the best fit is achieved when the system already at $\tau_i = 1$ fm/c expands in the transverse direction with a collective velocity field that reaches at the system border (at $r = R_i$) the value $v(R_i, \tau_i) \approx 0.34$ c. It may indicate that a noticeable contribution into buildup of transverse flow at RHIC energies is given at times earlier than 1 fm/c, possibly prethermal stages of evolution. It is interesting to note that hydrodynamic simulations [38] of heavy-ion collisions at RHIC energies also indicate the necessity of an initial (prehydrodynamic) transverse flow to better account for slopes of the observed spectra.

¹⁰Note that it is not only the absolute values but also the spectrum slopes that are affected by the values of $\mu_{s,j}$ because chemical potentials determine what part of particles are emitted from the *surface*, and these particles have, of course, different spectrum slopes than the ones emitted from the *volume* part of the freeze-out hypersurface.

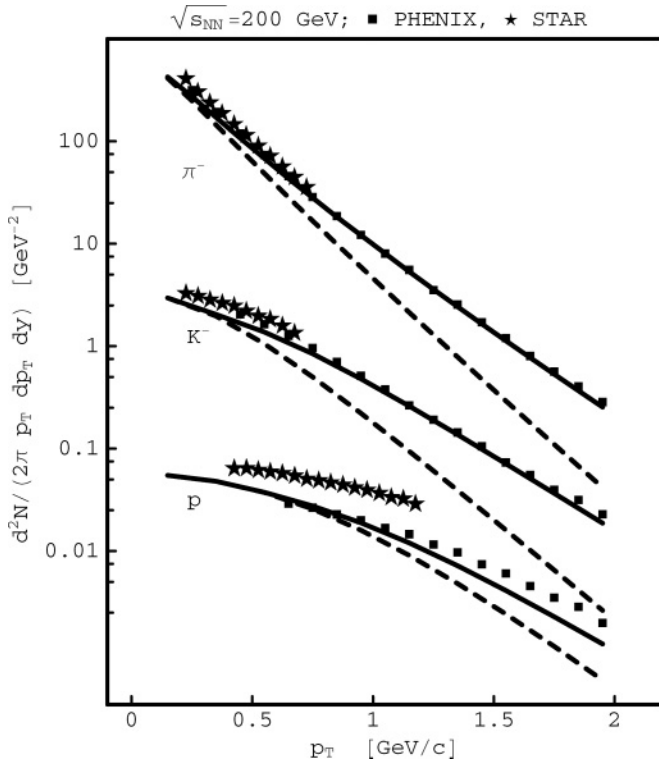


FIG. 2. Comparison of the single-particle momentum spectra measured by the PHENIX Collaboration with the model calculations performed for whole enclosed hypersurface (solid lines) and for shell-like part, see Fig. 1, solely (dashed lines). For convenience of plots location the measured p spectra are reduced in 100 times and K^- spectra in 8 times. The STAR data are not fitted and are presented for illustration.

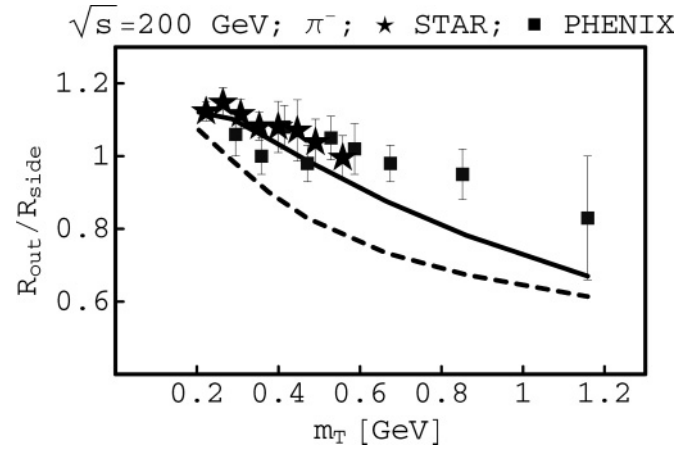


FIG. 4. Comparison of the measured by the STAR (stars) and PHENIX (boxes) Collaborations pion R_{out}/R_{side} ratios with model calculations performed for whole enclosed hypersurface (solid line) and for shelllike part only (dashed line).

The solid lines in Figs. 2–4 demonstrate the fit according to our model, and the dashed lines indicate the contributions to particle spectra and interferometry radii from *volume* freeze-out solely. The latter corresponds, in fact, to blast-wave model calculations with our *volume* freeze-out parameters and $\Delta\tau = 0$. The experimental data are taken from Refs. [39–41]. We used Boltzmann approximation for the distribution functions in the single-particle spectra and interferometry radii calculations for all particle species. One can see from Fig. 2 that *surface* emission leads to a noticeable enhancement of the single-particle momentum spectra in high p_T region, resulting thereby in an increase of the inverse spectra slope

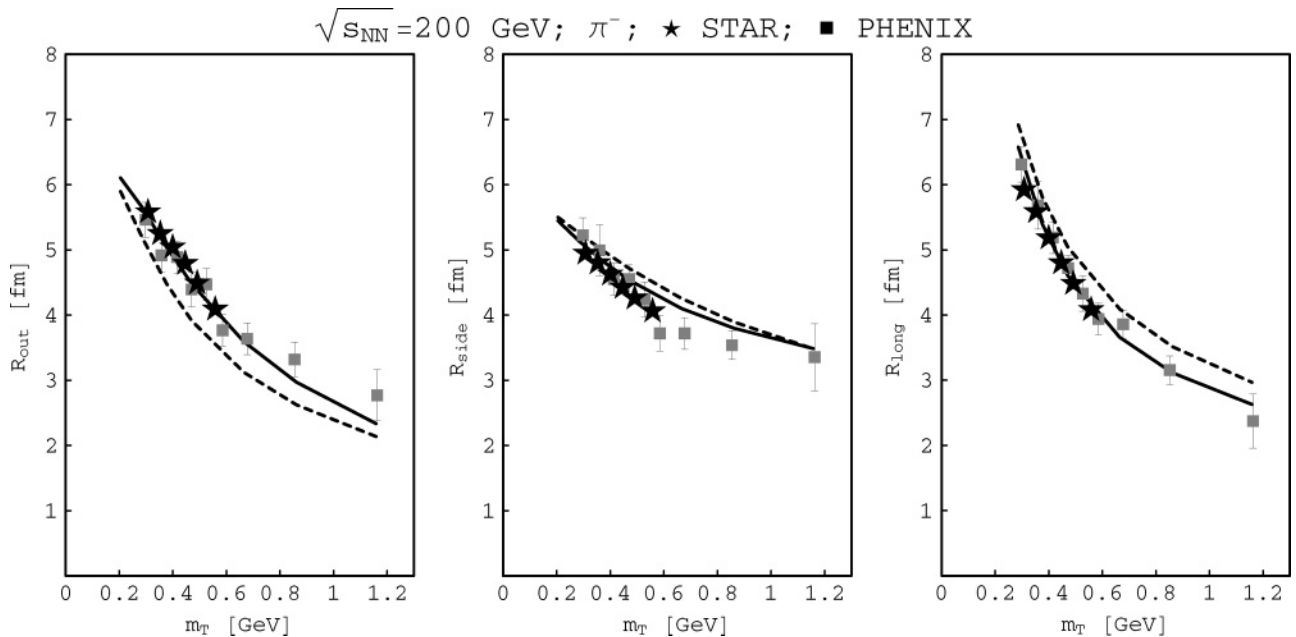


FIG. 3. Comparison of the pion source R_{out} , R_{side} , R_{long} radii measured by the STAR (stars) and PHENIX (boxes) Collaborations with model calculations performed for whole enclosed hypersurface (solid lines) and for shelllike part only (dashed lines). The PHENIX data are adjusted for most central bin (see the text for details).

or effective temperature. This happens because the particles with relatively low p_T are not emitted from the *surface* part of the freeze-out hypersurface that moves outwards and so their contribution to the spectra is suppressed, whereas the particles with sufficiently high p_T are liberated freely. This effect is taken into account, as discussed in the previous section, by means of multiplying the distribution functions by the step function, see Eq. (8), thus restricting the freeze-out to those particles for which the product $p^\mu n_\mu$ is positive. Note that in the blast-wave parametrization, which takes into account only *volume* emission, such a high effective temperature can be obtained only at the cost of a very high transverse flow ($\eta_T^{\max} \approx 0.9$ and so $v^{\max} \approx 0.7 c$, whereas in our parametrization $\eta_T^{\max} \approx 0.72$, $v^{\max} \approx 0.6 c$) at freeze-out [22], which seems less realistic and more difficult to reproduce in hydrodynamic models of the system evolution.

The Figs. 3 and 4 show our results for the interferometry radii of negative pions. Note that the interferometry radii are measured by the PHENIX Collaboration for 0%–30% centrality events at $\sqrt{s_{NN}} = 200$ GeV [41]. Therefore, to adjust the results of the PHENIX Collaboration to the most central 0%–5% centrality bin, we increase the corresponding interferometry radii by a factor calculated in accordance with the N_{part} dependence of the Bertsch-Pratt radius parameters found in Ref. [41]. As one can see from Fig. 3, the interplay between (i) a long emission time, $\tau_f - \tau_i$, which gives an increase of the R_{out} radius, and (ii) positive $r_{\text{out}} - t$ correlations at the *surface* part of the hypersurface where $d\tau_s/dr > 0$, which reduces the radius and provides a *moderate* increase of R_{out} as compared with the *volume* emission at constant τ .¹¹ The R_{side} radius is almost not affected by the *surface* emission.¹² As to R_{long} , it is less than in the *volume* emission case. The reason is that R_{long} is strongly affected by the value of the emission time τ [26] and, thereby, is reduced by the emission from early times $\tau < \tau_f$. This can explain an apparently low freeze-out value of τ in relativistic heavy-ion collisions if it is extracted assuming instantaneous *volume* emission at constant τ .

Figure 4 represents our result for the $R_{\text{out}}/R_{\text{side}}$ ratio. One can see that the *volume* blast-wave-like emission (at a constant τ) leads to a rather low $R_{\text{out}}/R_{\text{side}}$ ratio. The “extra” reduction of R_{out} is typical for a sharp freeze-out hypersurface with step density profile in the out-direction, $n(r) \sim \theta(R - r_{\text{out}})$ and the maximal velocity on the edge. The same boundary effect of the additional broadening of the correlation function at large momenta in the case of sharp steplike freeze-out in the long-direction have been found and described in detail in Ref. [42]. As one can see from Fig. 4, this effect becomes softer for an enclosed freeze-out hypersurface despite the fact that maximum velocity is also achieved at maximum transverse radius that the system occupies during its evolution. However, negative $t - r_{\text{out}}$ correlations can totally destroy the effect of relative reduction of R_{out} . That is why the positive

$t - r_{\text{out}}$ correlations in our model are very important to achieve a satisfactory description of the experimental data.

IV. SUMMARY

We have studied the effect of continuous particle emission on particle spectra and interferometry radii, based on hydro-inspired parametrization of the enclosed freeze-out hypersurface and distribution functions. Our model generalizes the “blast-wave” parametrization, which has difficulties in the fitting of the HBT radii and leads to too-large transverse velocities. We demonstrate that π^- , K^- , and p single-particle spectra and π^- interferometry radii at RHIC can be described by a physically reasonable set of parameters when a rather protracted emission (~ 9 fm/c) from the *surface* sector of the hypersurface that moves “outward” is taken into account. The phase-space distribution of particles emitted from the surface prior to the fireball breakup is similar to the local chemical equilibrium distribution with parameters rather close to the ones found at chemical freeze-out in RHIC Au+Au collisions. This could indicate a transformation of quark-gluon matter to hadron gas at the periphery of the system with subsequent hadronic emission just after such a transition from the boundary of the fireball during the whole time of the system’s hydro evolution.

Thereby, the simple physical arguments requiring the freeze-out hypersurface to be enclosed for finite expanding systems result in a successful description of hadronic spectra and interferometry radii. This means that particle emission from the early stages of fireball evolution has to be taken into account in advanced hydrodynamic models of $A+A$ collisions.¹³ A quantitative description of a continuous escaping of particles can be made, in particular, within the hydrokinetic approach to spectra formation proposed in Ref. [6].

ACKNOWLEDGMENTS

We are grateful to Stefan Mashkevich and Sergey Panitkin for careful reading of the manuscript and useful suggestions. The research described in this publication was made possible in part by Award No. UKP1-2613-KV-04 of the U.S. Civilian Research & Development Foundation for the Independent States of the Former Soviet Union (CRDF). The research was carried out within the scope of the ERG (GDRE): Heavy ions at ultrarelativistic energies—a European Research Group comprising IN2P3/CNRS, Ecole des Mines de Nantes, Universite de Nantes, Warsaw University of Technology, JINR Dubna, ITEP Moscow, and Bogolyubov Institute for Theoretical Physics, NAS of Ukraine. The work was also supported by NATO Collaborative Linkage grant PST.CLG.980086 and Fundamental Research State Fund of Ukraine, Agreement No. F7/209-2004.

¹¹The conclusion that a long-lived fireball can be compatible with HBT measurements is made also in Ref. [35].

¹²An independence of R_{side} on transport opacity was also found in a covariant transport model [18].

¹³The back reaction of evaporation of particles off the surface of the system created on the fluid dynamics was studied within boost-invariant hydrodynamics in Ref. [43].

- [1] RHIC Collaboration white papers: I. Arsene *et al.* (BRAHMS Collaboration), Nucl. Phys. **A757**, 1 (2005); B. B. Back *et al.* (PHOBOS Collaboration), *ibid.* **A757**, 28 (2005); J. Adams *et al.* (STAR Collaboration), *ibid.* **A757**, 102 (2005); K. Adcox *et al.* (PHENIX Collaboration), *ibid.* **A757**, 184 (2005).
- [2] U. Heinz, J. Phys. G **31**, S717 (2005); arXiv:nucl-th/0504011.
- [3] F. Cooper and G. Frye, Phys. Rev. D **10**, 186 (1974).
- [4] L. D. Landau, Izv. Akad. Nauk SSSR, Ser. Fiz. **17**, 51 (1953).
- [5] L. V. Bravina, K. Tywoniuk, and E. E. Zabrodin, J. Phys. G **31**, S989 (2005).
- [6] Yu. M. Sinyukov, S. V. Akkelin, and Y. Hama, Phys. Rev. Lett. **89**, 052301 (2002).
- [7] S. V. Akkelin, M. S. Borysova, and Yu. M. Sinyukov, Acta Phys. Hung. A: Heavy Ion Phys. **22**, 165 (2005).
- [8] K. A. Bugaev, Phys. Rev. C **70**, 034903 (2004).
- [9] L. P. Csernai, V. K. Magas, E. Molnar, A. Nyiri, and K. Tamosiunas, Eur. Phys. J. A **25**, 65 (2005).
- [10] S. Pratt, Phys. Rev. D **33**, 1314 (1986); Phys. Rev. C **49**, 2722 (1994).
- [11] G. F. Bertsch, Nucl. Phys. **A498**, 173 (1989); D. H. Rischke and M. Gyulassy, *ibid.* **A608**, 479 (1996); S. Soff, S. A. Bass, and A. Dumitru, Phys. Rev. Lett. **86**, 3981 (2001); S. Soff, S. A. Bass, D. H. Rischke, and S. Y. Panitkin, *ibid.* **88**, 072301 (2002).
- [12] H. Appelshauser, J. Phys. G **30**, S935 (2004); D. Magestro, *ibid.* **31**, 265 (2005).
- [13] U. Heinz, Nucl. Phys. **A721**, 30 (2003); M. Lisa, S. Pratt, R. Soltz, and U. Wiedemann, Ann. Rev. Nucl. Part. Sci. **55**, 357 (2005).
- [14] U. A. Wiedemann and U. Heinz, Phys. Rep. **319**, 145 (1999).
- [15] S. Pratt, Phys. Rev. Lett. **53**, 1219 (1984); G. Bertsch, M. Gong, and M. Tohyama, Phys. Rev. C **37**, 1896 (1988).
- [16] Z. W. Lin, C. M. Ko, and S. Pal, Phys. Rev. Lett. **89**, 152301 (2002); Z. W. Lin, C. M. Ko, B. A. Li, B. Zhang, and S. Pal, Phys. Rev. C **72**, 064901 (2005).
- [17] H. Heiselberg, Acta Phys. Hung. A: Heavy Ion Phys. **5**, 435 (1997).
- [18] D. Molnar and M. Gyulassy, Phys. Rev. Lett. **92**, 052301 (2004).
- [19] Yu. M. Sinyukov, Z. Phys. C **43**, 401 (1989).
- [20] K. A. Bugaev, Nucl. Phys. **A606**, 559 (1996); C. Anderlik, L. P. Csernai, F. Grassi, W. Greiner, Y. Hama, T. Kodama, Z. I. Lazar, V. K. Magas, and H. Stocker, Phys. Rev. C **59**, 3309 (1999).
- [21] K. Zalewski, Acta Phys. Pol. B **34**, 3379 (2003).
- [22] F. Retiere and M. A. Lisa, Phys. Rev. C **70**, 044907 (2004); B. Tomasik, Nucl. Phys. **A749**, 209 (2005).
- [23] H. Heiselberg and A. P. Vischer, Eur. Phys. J. C **1**, 593 (1998); L. McLerran, S. S. Padula, arXiv:nucl-th/0205028; S. S. Padula, Nucl. Phys. **A715**, 637 (2003).
- [24] P. F. Kolb and U. Heinz, in *Quark Gluon Plasma 3*, edited by R. C. Hwa and X. N. Wang (World Scientific, Singapore, 2004), p. 634.
- [25] J. D. Bjorken, Phys. Rev. D **27**, 140 (1983).
- [26] A. N. Makhlin and Yu. M. Sinyukov, Z. Phys. C **39**, 69 (1988); Yu. M. Sinyukov, Nucl. Phys. **A498**, 151c (1989); S. V. Akkelin and Yu. M. Sinyukov, Phys. Lett. **B356**, 525 (1995); Z. Phys. C **72**, 501 (1996).
- [27] S. V. Akkelin, P. Braun-Munzinger, and Yu. M. Sinyukov, Nucl. Phys. **A710**, 439 (2002).
- [28] Yu. M. Sinyukov and Iu. A. Karpenko, arXiv:nucl-th/0505041; arXiv:nucl-th/0506002, to be published in Acta Phys. Hung., 2006.
- [29] P. F. Kolb, Acta Phys. Hung. A: Heavy Ion Phys. **21**, 243 (2004).
- [30] M. Gyulassy and S. S. Padula, Phys. Lett. **B217**, 181 (1988).
- [31] P. Braun-Munzinger, J. Stachel, J. P. Wessels, and N. Xu, Phys. Lett. **B344**, 43 (1995); **B365**, 1 (1996); P. Braun-Munzinger, I. Heppe, and J. Stachel, *ibid.* **B465**, 15 (1999); P. Braun-Munzinger, D. Magestro, K. Redlich, and J. Stachel, *ibid.* **B518**, 41 (2001).
- [32] P. Braun-Munzinger, K. Redlich, and J. Stachel, in *Quark Gluon Plasma 3*, edited by R. C. Hwa and X. N. Wang (World Scientific, Singapore, 2004), p. 491.
- [33] S. V. Akkelin and Yu. M. Sinyukov, Phys. Rev. C **70**, 064901 (2004).
- [34] U. A. Wiedemann and U. Heinz, Phys. Rev. C **56**, 3265 (1997).
- [35] T. Renk, Phys. Rev. C **69**, 044902 (2004).
- [36] P. Braun-Munzinger, J. Stachel, and C. Wetterich, Phys. Lett. **B596**, 61 (2004).
- [37] M. Kaneta and N. Xu, arXiv:nucl-th/0405068.
- [38] P. F. Kolb and R. Rapp, Phys. Rev. C **67**, 044903 (2003).
- [39] S. S. Adler *et al.* (PHENIX Collaboration), Phys. Rev. C **69**, 034909 (2004).
- [40] J. Adams *et al.* (STAR Collaboration), Phys. Rev. Lett. **92**, 112301 (2004); J. Adams *et al.* (STAR Collaboration), Phys. Rev. C **71**, 044906 (2005).
- [41] S. S. Adler *et al.* (PHENIX Collaboration), Phys. Rev. Lett. **93**, 152302 (2004).
- [42] V. A. Averchenkov, A. N. Makhlin, and Yu. M. Sinyukov, Sov. J. Nucl. Phys. **46**, 905 (1987); Yad. Fiz. **46**, 1525 (1987).
- [43] A. Dumitru, C. Spieles, H. Stöcker, and C. Greiner, Phys. Rev. C **56**, 2202 (1997).